Adaptive Integrated Vehicle Control using Active Front Steering and Rear Torque Vectoring

D. Bianchi, A. Borri, G. Burgio, M. D. Di Benedetto, and S. Di Gennaro

***Abstract*— This work studies the combination of active front steering with rear torque vectoring actuators in an integrated controller to guarantee vehicle stability/trajectory tracking. Adaptive feedback technique has been used to design the controller. The feedback linearization is applied to cancel the nonlinearities in the input–output dynamics, leading to closed–loop dynamics diffeomorphic to a linear system. Parameter adaptation then is used to robustify the exact cancellation of the nonlinear terms. Some first results are here obtained, showing improved tracking performance when important parameters, like mass, inertia or tire stiffness, are affected by relevant estimation errors.**

I. Introduction

Today's vehicles are equipped with many electronically controlled systems, whose integration is rising in complexity with the increasing number of available customer features and technologies. A way to solve this integration problem can be the introduction of a hierarchical control structure, where all control commands are computed in parallel in one core algorithm, and where the control has to take into account the interactions among the vehicle subsystems, driver and vehicle.

The key element of integrated vehicle control is that the behavior of the various vehicle subsystems has to be coordinated, i.e. subsystems has to behave as cooperatively as possible in performing the desired vehicle functions. Clearly, the fully integrated controller will be more complex than the sum of the stand alone ones, but it will guarantee increased performance and robustness.

Active Safety Systems Integration is one of the main research topics in vehicle dynamics/control area. In order to maintain safe handling characteristics of the vehicle, several active system technologies (active braking, active steering, active differential, active suspension, etc.) have been developed. All these technologies modify the vehicle dynamics imposing forces or moments to the vehicle body, which can be generated in different ways (see e.g. [5], [7], [2], [1] and [8]). An important design factor to be considered in the standalone or integrated controller design is the actuator saturations, which limits the maximum obtainable performance. In an integrated control structure more power is available for control, thus potentially limiting the saturation occurrences.

In [5], a fully integrated vehicle controller with steering and brakes is proposed, using the exact feedback linearization method. The feedback linearization control method amounts to canceling the nonlinearities in a nonlinear system so that the closed–loop dynamics is in a linear form. The main drawback of this methodology is that performance deteriorates in the presence of parameter uncertainty or unmodeled dynamics.

Work partially supported by the Center of Excellence DEWS.

D. Bianchi, A. Borri, M. D. Di Benedetto, and S. Di Gennaro are with the Department of Electrical and Information Engineering, and Center of Excellence DEWS, University of L'Aquila, Poggio di Roio, 67040 L'Aquila, Italy. E-mail: {domenico.bianchi, alessandro.borri,mariadomenica.dibenedetto,stefano.digennaro}@univaq.it.

G. Burgio is with Ford–Forschungszentrum Aachen GmbH, Germany. E-mail: gburgio1@ford.com.

Other works on integrated active chassis systems propose integrated control systems with active front steering and direct yaw moment control based on fuzzy logic control [7]. In [2], an active steering control design method is proposed in order to preserve vehicle stability in extreme handling situations. Active chassis control systems, guaranteeing the stability performance in the presence of parameter uncertainty/variation, can be found in [1] and [8], where issues on robustness of active steering systems are addressed.

In this paper we propose a robust integrated chassis control system for a rear–wheel drive vehicle, equipped with Active Front Steering (AFS) and Rear Torque Vectoring (RTV) devices, in the presence of parameter uncertainties. While the AFS provides additional steering angle over the driver defined one, the RTV gives asymmetric left/right wheel torque on the rear axle.

Another goal of the paper is to evaluate the possibility of combining AFS with RTV to guarantee vehicle stability/trajectory tracking in a variety of situations, not only in the presence of deviation of the vehicle parameters from the nominal values, but also in situations of rapid variability of road conditions (dry, wet, iced). This is accomplished by using the adaptive feedback linearization technique, where parameter adaptation is used to robustify the exact cancellation of nonlinear terms. Such a method shows an improvement of the robustness and of the control performance, if compared with the exact linearization, with a limited additional computation effort.

The paper is organized as follows. In Section II, the mathematical model of a vehicle is recalled, and the control problem is set. In Section III, the adaptive feedback linearization technique is applied, and the adaptive controller is designed. In Section IV, the proposed controller is tested with simulations. Some comments conclude the paper.

II. Mathematical Model and Problem Setting

The vehicle motion can be in general described as a rigid body moving in the free space, with 6 degrees of freedom, connected with the ground surface through tires and suspensions. This results in a model with high non–linear behavior and high coupling effects. For simplicity, we consider the model of a rear–wheel drive vehicle, which has less coupling effects between the directional and traction actuators. The actuators considered in this work are

- Active Front Steer (AFS), which imposes an incremental steer angle on top of the driver's input. The control is then actuated through the front axle tire characteristic.
- Rear Torque Vectoring (RTV), which distributes the torque in the rear axle, usually to improve vehicle handling and stability. The control is then actuated through the rear axle tire characteristics.

The mathematical model is derived under the following assumptions, which are verified in a large number of situations, and which mitigate the complexity of the vehicle dynamics

- The vehicle moves on a horizontal plane;
- The longitudinal velocity is constant, so that vehicle shaking/pitch motions can be neglected;
- The vehicle has stiff suspensions, so that the vehicle roll can be neglected;
- The steering system is rigid, so that the angular position of the front wheels is uniquely determined by the steering wheel position;
- The wheels masses are much lower than the vehicle one, so the steering action does not affect the position of the centre of mass of the entire vehicle;
- The vehicle takes large radius bends and the road wheel angles are "small" (less than 10°), i.e. the bend curve radius is much higher than the vehicle width;
- The aerodynamic resistance and the wind lateral thrust are not considered;
- The tire vertical loads are constant;
- The actuators are ideally modelled and their dynamics are neglected.

These assumptions are quite standard in vehicle control. Moreover, it is relatively common to decouple the cornering dynamics (involving velocities acting on the horizontal plane) from the dynamics of shaking, roll and pitch (e.g. connected to the design of suspensions).

As a consequence of the previous assumptions, the height of each point of the vehicle is kept constant, and the vehicle motion is planar. The resulting model has two degrees of freedom

$$\begin{aligned} m(\dot{v}_y + v_x\omega_z) &= \mu(F_{y,f} + F_{y,r}) \\ J\dot{\omega}_z &= \mu(F_{y,f}l_f - F_{y,r}l_r) + M_c \end{aligned} \tag{1}$$

where the state variables are the vehicle lateral velocity v_y (m/s), and the vehicle yaw velocity ω_z (rad/s), and where we have denoted

m	vehicle mass (kg)
J	vehicle inertia momentum ($\mathrm{kg\,m^2}$)
v_x	vehicle longitudinal velocity (m/s)
l_f, l_r	front, rear vehicle lengths from the center of gravity (m)
$F_{y,f}, F_{y,r}$	front, rear tire lateral forces (N)
M_c	RTV yaw moment (N m)
μ	tire–road friction coefficient (dimensionless).

Despite its simplicity, the vehicle model, derived under these simplifying assumptions, well captures the real vehicle major characteristics of interest for the controller design (e.g. the steady state and dynamic responses of the yaw rate, lateral acceleration, lateral velocity). The influence of environmental disturbances (e.g. wind lateral thrusts) have been taken into account in simulations. The front/rear lateral forces

$$F_{y,f} = F_{y,f}(\alpha_f), \quad F_{y,r} = F_{y,r}(\alpha_r)$$

depend on the front/rear tire slip angles (rad)

$$\alpha_f = \delta - \frac{v_y + l_f\omega_z}{v_x}, \quad \alpha_r = -\frac{v_y - l_r\omega_z}{v_x}$$

with $\delta = \delta_c + \delta_d$ the road wheel angle (rad), sum of the AFS angle δ_c (rad) and the driver angle δ_d (rad).

The tire lateral behavior can be represented by some functions describing the dependence on the slip angle (see, for instance [11]). The tires determine a force in the direction of the slip angles, which contrasts the drift of the wheel, but this force decreases after a certain value of the slip angle, as in the following function

$$F_{y,f}(\alpha_f) = C_{y,f}F_{yn,f}(\alpha_f)$$
$$F_{y,r}(\alpha_r) = C_{y,r}F_{yn,r}(\alpha_r)$$

where

$$F_{yn,f}(\alpha_f) = \sin(A_{y,f}\arctan(B_{y,f}\alpha_f))$$
$$F_{yn,r}(\alpha_r) = \sin(A_{y,r}\arctan(B_{y,r}\alpha_r))$$

are normalized tire functions, and with $A_{y,f}$, $B_{y,f}$, $C_{y,f}$, $A_{y,r}$, $B_{y,r}$, $C_{y,r}$ positive experimental parameters.

The control inputs are the AFS angle δ_c and the RTV yaw moment M_c. This latter determines differential torques at the rear right/left wheels $T_{AD} = \pm r_w M_c/2d$, where $2d$ is the vehicle track and r_w is the wheel radius. The former can be computed inverting the function $F_{y,f}$. This can be done up to the tyre saturation point $\alpha_{f,\mathrm{sat}}$ and saturating the inverse function elsewhere, i.e.

$$\delta_c = \begin{cases} -\delta_d + \dfrac{v_y + l_f\omega_z}{v_x} + F_{y,f}^{-1}(F_0), & |F_0| \le F_{y,f}(\alpha_{f,\mathrm{sat}}) \\ -\delta_d + \dfrac{v_y + l_f\omega_z}{v_x} + \alpha_{f,\mathrm{sat}}, & \text{otherwise} \end{cases}$$

for a given value F_0. This allows considering as control input the difference

$$\Delta_{y,f} = F_{yn,f}(\alpha_f) - F_{yn,f}(\alpha_{f,d})$$
$$\alpha_{f,d} = \delta_d - \frac{v_y + l_f\omega_z}{v_x}$$

instead of δ_c, so that equations (1) become

$$\begin{aligned} m(\dot{v}_y + v_x\omega_z) &= \mu\Big(C_{y,f}F_{yn,f}(\alpha_f) + C_{y,r}F_{yn,r}\Big) \\ &\quad + \mu C_{y,f}\Delta_{y,f} \\ J\dot{\omega}_z &= \mu\Big(C_{y,f}F_{yn,f}(\alpha_f)l_f - C_{y,r}F_{yn,r}l_r\Big) \\ &\quad + \mu C_{y,f}l_f\Delta_{y,f} + M_c. \end{aligned} \tag{2}$$

The vehicle dynamics (2) are represented by the state space (input–affine) model

$$\dot{x} = f(t,x) + bu \tag{3}$$

where

$$x = \begin{pmatrix} v_y \\ \omega_z \end{pmatrix} \in \mathbb{R}^2, \quad u = \begin{pmatrix} \Delta_{y,f} \\ M_c \end{pmatrix} \in \mathbb{R}^2$$

with f the smooth function

$$\begin{aligned} f(t,x) &= \begin{pmatrix} \phi_1 \\ \phi_2 \end{pmatrix} \\ \phi_1 &= -v_x\omega_z + \frac{\mu}{m}\Big(C_{y,f}F_{yn,f}(v_y,\omega_z,\delta_d) \\ &\qquad + C_{y,r}F_{yn,r}(v_y,\omega_z)\Big) \\ \phi_2 &= \frac{\mu}{J}\Big(C_{y,f}F_{yn,f}(v_y,\omega_z,\delta_d)l_f \\ &\qquad - C_{y,r}F_{yn,r}(v_y,\omega_z)l_r\Big) \end{aligned}$$

and b the constant matrix

$$b = \begin{pmatrix} \dfrac{\mu C_{y,f}}{m} & 0 \\ \dfrac{\mu C_{y,f}l_f}{J} & \dfrac{1}{J} \end{pmatrix}.$$

In $F_{yn,f}, F_{yn,r}$ we put in evidence the dependence on v_y, ω_z, and $\delta_d(t)$.

The control problem is the following: Given the system (3), and two target functions $v_{y,r}(t)$, $\omega_{z,r}(t)$ for lateral velocity and yaw rate, find a control law $u(x)$ ensuring global asymptotic tracking, i.e.

$$\lim_{t\to\infty} v_y = v_{y,r}, \quad \lim_{t\to\infty} \omega_z = \omega_{z,r}$$

for all initial conditions $v_y(0)$, $\omega_z(0)$, and in presence of uncertainties on the parameters. The target or reference signals $v_{y,r}(t)$, $\omega_{z,r}(t)$ are desired behaviors of the vehicle, and are bounded functions with bounded derivatives. In the following we will assume that also the driver angle δ_d is bounded.

III. Adaptive feedback linearization

The following parameters of the vehicle dynamics can be known with a certain uncertainty or may be subject to variations

- the tire–road friction coefficient μ;
- the vehicle mass m and moment of inertia J;
- the force factors $C_{y,f}$, $C_{y,r}$ of the front/rear axles.

In this section an adaptive linearizing controller which takes into account these uncertainties is designed. For, the dynamics (2) can be rewritten as follows

$$\begin{aligned}
\dot v_y &= -v_x\omega_z + \frac{\mu C_{y,f}}{m}F_{yn,f}(v_y,\omega_z,\delta_d)\\
&\quad + \frac{\mu C_{y,r}}{m}F_{yn,r}(v_y,\omega_z) + \frac{\mu C_{y,f}}{m}\Delta_{y,f}\\
\dot\omega_z &= \frac{\mu C_{y,f} l_f}{J}F_{yn,f}(v_y,\omega_z,\delta_d)\\
&\quad - \frac{\mu C_{y,r} l_r}{J}F_{yn,r}(v_y,\omega_z) + \frac{\mu C_{y,f} l_f}{J}\Delta_{y,f} + \frac{1}{J}M_c.
\end{aligned} \tag{4}$$

Defining

$$\theta_1 = \frac{\mu C_{y,f}}{m}, \quad \theta_2 = \frac{\mu C_{y,r}}{m}, \quad \theta_3 = \frac{\mu C_{y,f}}{m}$$
$$\theta_4 = \frac{\mu C_{y,f} l_f}{J}, \quad \theta_5 = \frac{\mu C_{y,r} l_r}{J} \quad \theta_6 = \frac{\mu C_{y,f} l_f}{J}, \quad \theta_7 = \frac{1}{J}.$$

equations (4) rewrite

$$\begin{aligned}
\dot v_y &= -v_x\omega_z + \theta_1 F_{yn,f} + \theta_2 F_{yn,r} + \theta_3 \Delta_{y,f}\\
\dot\omega_z &= \theta_4 F_{yn,f} - \theta_5 F_{yn,r} + \theta_6\Delta_{y,f} + \theta_7 M_c.
\end{aligned}$$

or, in compact form,

$$\dot x = f_0(x) + f_1^T(t,x)\theta + B(\theta)u \tag{5}$$

where

$$f_0(x) = \begin{pmatrix} -v_x\omega_z \\ 0 \end{pmatrix}, \quad B(\theta) = \begin{pmatrix} \theta_3 & 0 \\ \theta_6 & \theta_7 \end{pmatrix}$$

$$f_1^T(t,x) = \begin{pmatrix} F_{yn,f} & F_{yn,r} & 0 & 0 & 0 & 0 & 0 \\ 0 & 0 & 0 & F_{yn,f} & -F_{yn,r} & 0 & 0 \end{pmatrix}.$$

If θ is known, we know that the linearizing and decoupling control law [6]

$$u(t,x,\theta) = \Big(B(\theta)\Big)^{-1}\Big(v - f_0(x) - f_1(t,x)\theta\Big) \tag{6}$$

yields to the linear input–state dynamics $\dot x = v$, where the new input v can be chosen as

$$\begin{aligned}
v_1 &= \dot v_{y,r} - k_{p1}\big(v_y - v_{y,r}\big)\\
v_2 &= \dot\omega_{z,r} - k_{p2}\big(\omega_z - \omega_{z,r}\big)
\end{aligned}$$

$k_{p1}, k_{p2} > 0$, i.e.

$$\begin{aligned}
&v = \dot x_r + Ae\\
&A = \begin{pmatrix} -k_{p1} & 0 \\ 0 & -k_{p2} \end{pmatrix}, \quad e = \begin{pmatrix} v_y - v_{y,r} \\ \omega_z - \omega_{z,r} \end{pmatrix}
\end{aligned} \tag{7}$$

ensuring the exponential tracking of the bounded references with bounded derivatives. Note that A is Hurwitz. Note also that the control (6) exists when $\theta_3\theta_7 \neq 0$, i.e. when $\mu, C_{y,f} \neq 0$, as in real cases.

If θ is uncertain, the adaptive linearization technique can be exploited [13], in which θ is replaced with its estimate $\hat\theta$, yielding to the control

$$\hat u(t,x,\hat\theta) = \begin{pmatrix} \hat u_1 \\ \hat u_2 \end{pmatrix} = \Big(B(\hat\theta)\Big)^{-1}\Big(v - f_0(x) - f_1(t,x)\hat\theta\Big) \tag{8}$$

and an appropriate adaption rule $\dot{\hat\theta}$ is designed. Since the control (8) exists when $\hat\theta_3\hat\theta_7 \neq 0$, such an adaptation rule has to constrain these estimations to positive values. This mathematical condition does not have a direct correspondence on the estimates of the real parameters μ, $C_{y,f}$, $C_{y,r}$, m, J, since from $\hat\theta_1, \cdots, \hat\theta_7$ it is not possible to determine univocally estimations of the real parameters.

The adaption scheme will improve the performance of (6) in the presence of parameter uncertainty, ensuring the asymptotic stability of the tracking errors, as shown in what follows. Since

$$v = f_0(x) + f_1(t,x)\hat\theta + B(\hat\theta)\hat u(t,x,\hat\theta)$$

applying (8) to (5) one gets

$$\dot x = v + f_1^T(t,x)\tilde\theta + B(\tilde\theta)\hat u(t,x,\hat\theta) = v + M^T(t,x,\hat\theta)\tilde\theta$$

where $\tilde\theta = \theta - \hat\theta$, and

$$M(t,x,\hat\theta) = f_1^T(t,x) + f_2^T(t,x,\hat\theta)$$

$$f_2^T = \begin{pmatrix} 0 & 0 & \hat u_1 & 0 & 0 & 0 & 0 \\ 0 & 0 & 0 & 0 & 0 & \hat u_1 & \hat u_2 \end{pmatrix}.$$

Considering the expression (7) of the new input, we can rewrite

$$\dot e = Ae + M^T(t,x,\hat\theta)\tilde\theta.$$

To study the stability of the origin of the feedback system (5), (8), (7), let us consider the candidate Lyapunov function

$$V(e,\tilde\theta) = \frac{1}{2}e^T P e + \frac{1}{2}\tilde\theta^T \Gamma^{-1}\tilde\theta$$

with $P = P^T > 0$ solution of the equation

$$PA + A^T P = -2Q$$

for a chosen $Q = Q^T > 0$. Differentiating along the trajectories of the system, one gets

$$\dot V = e^T P\dot e + \tilde\theta^T\Gamma^{-1}\dot{\tilde\theta} = -e^T Q e + \tilde\theta^T\Big(M(t,x,\hat\theta)Pe - \Gamma^{-1}\dot{\hat\theta}\Big)$$

since $\dot\theta = 0$. Therefore, setting

$$\dot{\hat\theta} = \Gamma M(t,x,\hat\theta)Pe$$

one gets

$$\dot V = -e^T Q e \le -\lambda^Q_{\min}\|e\|^2 \tag{9}$$

with $\lambda^Q_{\min}$ the minimum eigenvalue of Q. This ensures that the tracking error e and the parameter error $\tilde\theta$ are bounded, i.e. $e, \tilde\theta \in L_\infty$.

To prove the convergence of e to zero, integrating (9) from t_0 to t one obtains

$$V(t) - V(t_0) \leq -\lambda_{\min}^{Q} \int_{t_0}^{t} \|e(\tau)\|^2 \, d\tau$$

and since $V(t) > 0$

$$\int_{t_0}^{t} \|e(\tau)\|^2 \, d\tau \leq \frac{V(t_0) - V(t)}{\lambda_{\min}^{Q}} \leq \frac{V(t_0)}{\lambda_{\min}^{Q}}.$$

Therefore, for $t \to \infty$

$$\int_{t_0}^{\infty} \|e(\tau)\|^2 \, d\tau \leq \frac{V(t_0)}{\lambda_{\min}^{Q}}$$

i.e. $e \in L_2$. Finally, to prove that $\|e\|^2$ is uniformly continuous, one notes that

$$\dot{e} = Ae + M^T(t, x, \hat{\theta})\tilde{\theta} \in L_\infty$$

since $e, \tilde{\theta} \in L_\infty$, as already noted, and $x_r, \dot{x}_r \in L_\infty$ as well as $\delta_d \in L_\infty$, by assumption. Applying Barbalat lemma [9], one deduces that

$$\lim_{t \to \infty} e = 0$$

i.e. the tracking error converges asymptotically to zero. It is worth noting that the present control scheme does no ensures, in general, the convergence of the estimated parameters $\hat{\theta}$ to the real values θ.

IV. Simulation results

Simulations have been carried out to evaluate the performance of the adaptive integrated control of AFS/RTV. The adaptive linearizing controller has been compared with the non adaptive version. The following test maneuvers have been considered

1. A step steer of 80° performed at 100 km/h, with abrupt variation of the friction coefficient;
2. A step steer of 80° performed at 100 km/h, with abrupt variation of the friction coefficient, variation of some of the tire parameters, and wind blast.

The real parameters of the system are

$$m = 1870 \text{ kg}, \quad J = 3630 \text{ kg m}^2, \quad \mu = 1$$
$$C_{y,f} = 8494, \quad C_{y,r} = 8129$$

and $l_f = 1.37$ m, $l_r = 1.52$ m, so that

$$\theta_1 = 4.54, \quad \theta_2 = 4.34, \quad \theta_3 = 0.00053, \quad \theta_4 = 3.2$$
$$\theta_5 = 3.4, \quad \theta_6 = 0.00037, \quad \theta_7 = 0.00027.$$

In all simulations the friction coefficient is subject to variations and measurement noises, simulated by an additive white Gaussian noise, as shown in Figure 1, where a sudden change of the friction coefficient occurs at $t = 2$ s.

The nominal parameters, used for the controller, are

$$m_0 = 1700 \text{ kg}, \quad J_0 = 3300 \text{ kg m}^2, \quad \mu_0 = 1$$
$$C_{y,f,0} = 8941, \quad C_{y,r,0} = 8556.$$

Figures 2–6 refer to the first test maneuver. Both the non adaptive and the adaptive controllers ensure the vehicle stability, namely that the vehicle state variables remain bounded, but the adaptive control system shows a better performance. Figures 2–3 show the

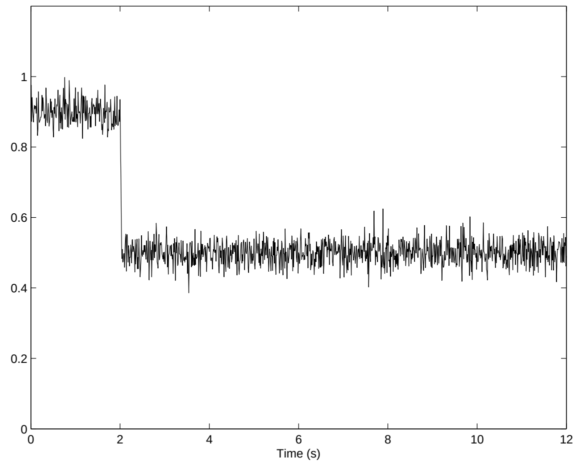

Fig. 1. Friction coefficient [dimensionless]

performance of the two integrated control in tracking desired lateral velocity and yaw rate: the adaptive control leads to zero state errors after a short transient, while the error on the estimated parameters doesn't go to zero, in accordance with the theory. Referring to Figure 4, in both the non–adaptive and the adaptive case, the AFS's angles agree with the input of the driver, but the adaptive control applies a lower value when grip coefficient decreases, as one could desire. On the other hand, the differential torques at the beginning are consistent with the driver input, but then they become opposite to it. Figure 5 shows the better performance of the adaptive control over the non–adaptive, in terms of smaller tracking error. It is worth noting that the controller ensures the tracking of the lateral and angular velocity references, not trajectory tracking; the transient errors in the tracked velocities results in a drift in the vehicle trajectory. During the maneuver, the vehicle reaches high value of the lateral acceleration, approximately 0.8 g (see Figure 6).

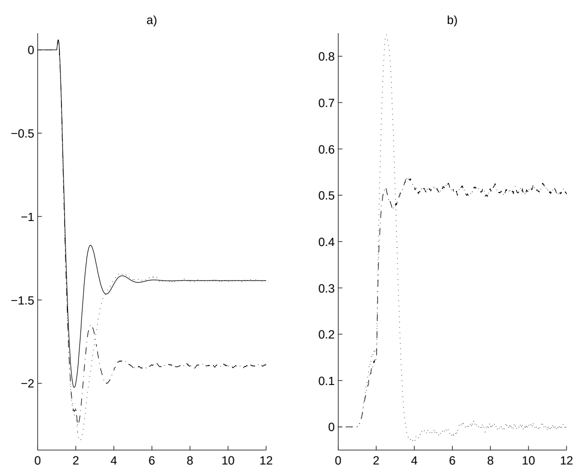

Fig. 2. Step steer, first maneuver: a) Lateral velocity: reference (solid), adaptive control (dotted), non adaptive control (dashdot) [m/s]; b) lateral velocity errors: adaptive control (dotted), non adaptive control (dashdot) [m/s]

In the second simulation the robustness of the adaptive controller is tested against unmodeled parameter variations. In fact, the maneuver is the same, but we have considered variations in the parameters $A_{y,f}$, $B_{y,f}$, $A_{y,r}$, $B_{y,r}$ appearing in the tire

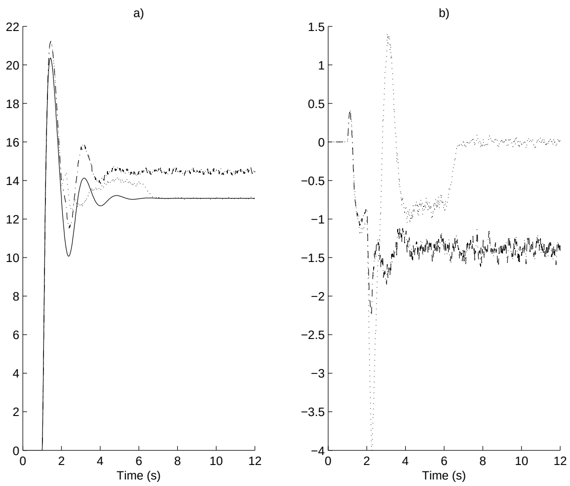

Fig. 3. Step steer, first maneuver: a) Yaw rate: reference (solid), adaptive control (dotted), non adaptive control (dashdot) [deg/s]; b) yaw rate errors: adaptive control (dotted), non adaptive control (dashdot) [deg/s]

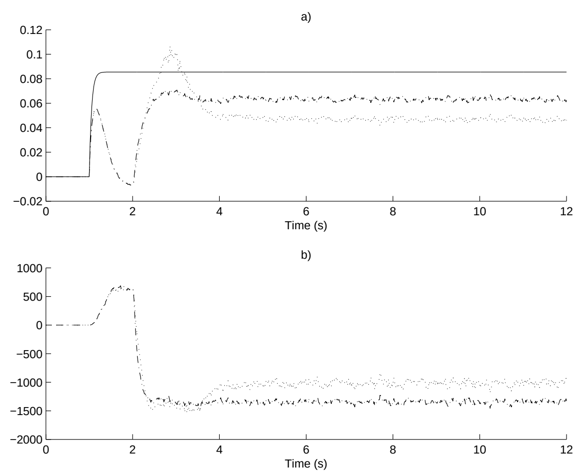

Fig. 4. Step steer, first maneuver: a) Road wheel angles: δ_d (solid), δ_c adaptive control (dotted), non adaptive control (dashdot) [rad]; b) Differential Torque: adaptive control (dotted), non adaptive control (dashdot) [N m]

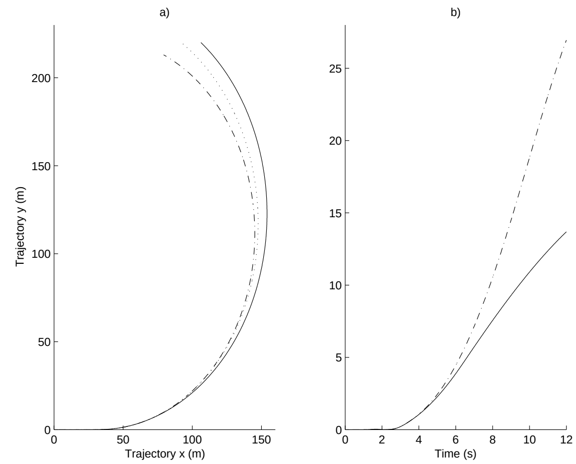

Fig. 5. Step steer, first maneuver: a) Trajectory in the plane: reference (solid), adaptive control (dotted), non adaptive control (dashdot); b) Trajectory error: adaptive control (solid), non adaptive control (dashdot) [m]

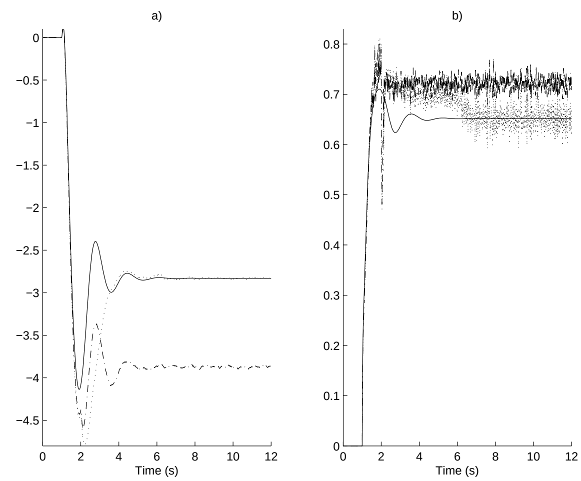

Fig. 6. Step steer, first maneuver: a) Vehicle slip angle: reference (solid), adaptive control (dotted), non adaptive control (dashdot) [deg] b) Lateral Acceleration: reference (solid), adaptive control (dotted), non adaptive control (dashdot) [g]

characteristics. Variations of -10%, 30%, 40% and -18% of these parameters have been considered. Moreover, to test the capability of rejecting unmodeled disturbances, a wind blast of 800 N, at $t = 5$ s and up to $t = 10$ s, is considered, acting on the rear axle and pointing to the left–hand side of the vehicle. The results are shown in Figures 7–11. Due to the parameter variations, the vehicle with the non–adaptive control turns more than expected (see Figure 10) and the lateral velocity error is not zeroed. On the contrary, the adaptive control leads to zero errors after a short transient, and ensures an effective rejection of the disturbance due to the wind blast. Figure 9 shows that the AFS's angles agree with input driver, while differential torques are opposite to it. Finally, the action of adaptive control is lower, and this ensures good tracking results.

V. Conclusions

In this paper an integrated chassis control system has been proposed to improve vehicle handling and stability. The choosen actuators have been active steering and rear torque vectoring, even if the proposed approach can be generalized and extended to other actuator configurations. It has been shown that AFS and RTV actuators can be effectively used in conjunction, and an integrated controller design has been proposed for a vehicle in the presence of parameter uncertainties, ensuring the tracking of desired references, and the robustness of the control system for both parameter uncertainties and unmodeled dynamics. Future work will deal with the comparison of the proposed controller with other existing controllers.

References

[1] J. Ackermann, J. Guldner, R. Steinhausner and V. Utkin, Linear and nonlinear design for robust automatic steering, *IEEE Transactions on Control System Technology*, Vol. 3, No. 1, pp. 132–143, 1995.

[2] S. C. Baslamisli, I. Polat and I. E. Kose, Gain Scheduled Active Steering Control Based on a Parametric Bicycle Model, *IEEE Intelligent Vehicles Symposium*, pp. 1168–1173, 2007.

[3] E. Esmailzadeh, A. Goodarzi, and G. R. Vossoughi, Optimal Yaw Moment Control Law for Improved Vehicle Handling, *Mechatronics*, Vol. 13, No. 7, pp. 659–675, 2003.

[4] M. Guiggiani, *Dinamica del Veicolo*, 2^{nd} Ed., Città Studi Edizioni, in Italian, Torino, 2007.

[5] G. Burgio, P. Zegelaar, Integrated vehicle control using steering and brakes, *International Journal of Control*, Vol. 79, No. 2, pp. 162–169, 2006.

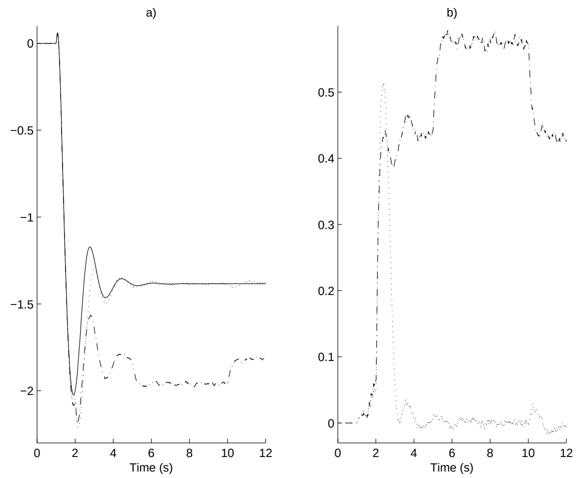

Fig. 7. Step steer, second maneuver: a) Lateral velocity: reference (solid), adaptive control (dotted), non adaptive control (dashdot) [m/s]; b) lateral velocity errors: adaptive control (dotted), non adaptive control (dashdot) [m/s]

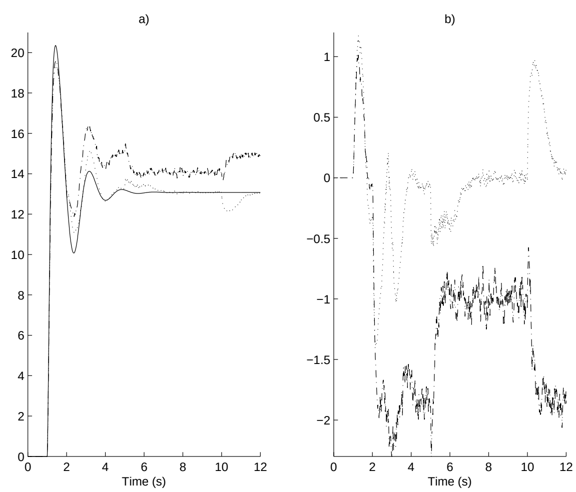

Fig. 8. Step steer, second maneuver: a) Yaw rate: reference (solid), adaptive control (dotted), non adaptive control (dashdot) [deg/s]; b) yaw rate errors: adaptive control (dotted), non adaptive control (dashdot) [deg/s]

[6] A. Isidori, *Nonlinear Control System: An Introduction*, Springer Verlag, London, Third Edition, 1995.

[7] R. Karbalaei, A. Ghaffari, R. Kazemi and S. H. Tabatabaei, Design of an Integrated AFS/DYC based on fuzzy logic control, *IEEE International Conference on Volume Vehicular Electronics and Safety*, pp. 1–6, 2007.

[8] S. Malan, M. Taragna, P. Borodani, and L. Gortan, Robust performance design for a car steering device, *Proceedings of the … IEEE Conference on Decision and Control World Congress*, pp. 474–479, 1994.

[9] R. Marino, and P. Tomei, *Nonlinear control design: geometric, adaptive and robust*, Prentice Hall International, Hertfordshire (UK), 1996.

[10] H. Pacejka, Tire and vehicle dynamics, *SAE*, Warrendale, 2002.

[11] H. B. Pacejka, Tyre and Vehicle Dynamics, Elsevier Butterworth–Hein, 2005.

[12] R. Rajamani, Vehicle Dynamics and Control, *Mechanical Engineering Series*, Springer–Verlag, 2006.

[13] S. Sastry, A. Isidori, Adaptive Control of Linearizable Systems, *IEEE Transactions on Automatic Control*, Vol. 34, No. 11, pp. 1123–1131, 1989.

[14] P. Setlur, J. R. Wagner, D. M. Dawson, and D. Braganza, A Trajectory Tracking Steer–by–Wire Control System for Ground Vehicles, *IEEE Transactions on Vehicular Technology*, Vol. 55, No. 1, pp. 76–85, 2006.

[15] J.-J. E. Slotine, and W. Li, *Applied Nonlinear Control*, Prentice Hall, Englewood Cliffs, New Jersey, 1991.

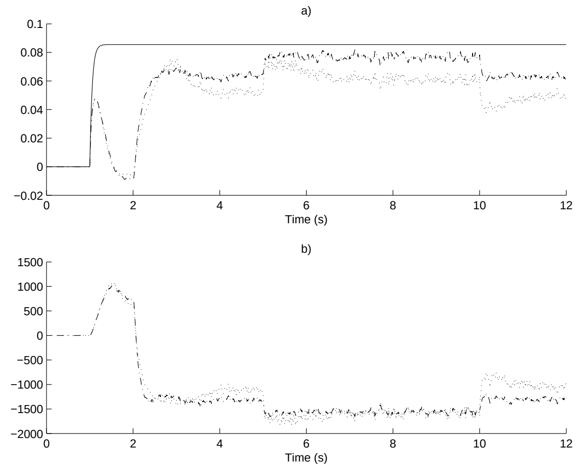

Fig. 9. Step steer, second maneuver: a) Road wheel angles: δ_d (solid), δ_c adaptive control (dotted), non adaptive control (dashdot) [rad]; b) Differential Torque: adaptive control (dotted), non adaptive control (dashdot) [N m]

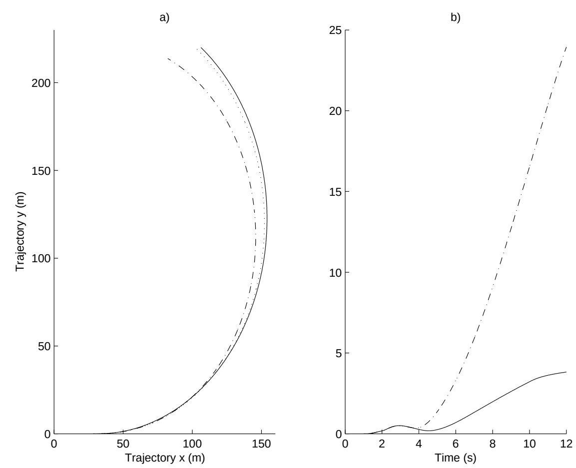

Fig. 10. Step steer, second maneuver: a) Trajectory in the plane: reference (solid), adaptive control (dotted), non adaptive control (dashdot); b) Trajectory error: adaptive control (solid), non adaptive control (dashdot) [m]

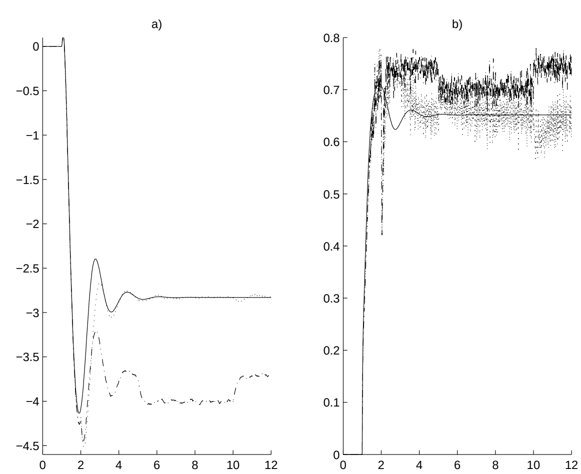

Fig. 11. Step steer, second maneuver: a) Vehicle slip angle: reference (solid), adaptive control (dotted), non adaptive control (dashdot) [deg] b) Lateral Acceleration: reference (solid), adaptive control (dotted), non adaptive control (dashdot) [g]